ADAPTIVE GUN BARREL VIBRATION ABSORBER

Andrew Littlefield and Eric Kathe[1]

[1]*US Army, TACOM-ARDEC Benét Laboratories, Watervliet Arsenal, NY 12189-4050*

Gun barrel vibrations lead to dispersion in the shot patterns. Thus, reducing these vibrations should lead to increased accuracy. Since the muzzle is the anti-node for all vibration modes and its vibrations have the greatest effect on shot dispersion, it is the obvious location to attempt to dampen the vibrations. A model of the gun barrel was created in MATLAB® and verified by modal impact testing. Modal impact testing was done for the barrel alone and for three different muzzle brake vibration absorber configurations. Significant reductions in muzzle vibrations were achieved using the vibration absorber. Methods of making the vibration absorber adaptive and models of such a system are presented.

INTRODUCTION

Vibration of the gun barrel in rapid-fire systems leads to dispersion in the shot patterns. The wider the dispersion the more rounds required to effect the desired damage on the enemy. An intuitive way to reduce this shot dispersion is to reduce the vibrations of the barrel. The end of the barrel is the anti-node for all vibration modes and its vibrations have the greatest affect on shot dispersion, so it is the obvious location to attempt to dampen the vibrations. This work focuses on doing just that.

The system under study in this work is the 25mm M242 Bushmaster chain gun. It is part of the M2A3 and M3A3 Bradley Fighting Vehicle Systems and is designed to engage and defeat armored vehicles as well as provide suppression fire. When engaging armored enemy assets, such as armored personnel carriers, accuracy is extremely important. The M242 fires five different rounds, M791, M792, M793, M910, and M919, though only the M793 training round was used in the tests.

A gun barrel vibration absorber has been previously designed [1] and tested [2] for use on the 120mm XM291 tank gun [3]. This design had the absorber as part of the gun's thermal shroud. The present effort differs in its unique location, application to rapid-fire gun systems and its possible dual use as part of a fuse setting system.

The vibration absorber being considered is of the proof mass actuator type and is mounted unto the muzzle brake. This allows for the absorber to be easily mounted and removed with the muzzle brake while still acting at the barrel location of greatest vibration activity. Addition of the absorber reshapes the frequency response by moving the resonant modes and zeros. This shifting effectively rejects the vibrational energy. Also the motion of the absorber enhances the dissipation of this energy.

First, the barrel is modeled in MATLAB® using a finite element approach [4]. The Euler-Bernoulli finite element technique is used to generate second order equations of motion of the barrel as a non-uniform beam. These are then converted to the first-order state space domain and transformed into the frequency domain. Predictions for the mode shapes and resonant

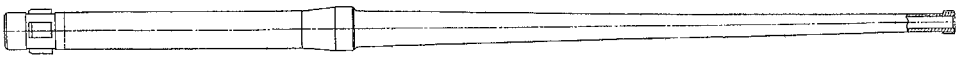

FIGURE 1. M242 BARREL

frequencies are generated. After completing the model, it is verified by performing modal impact testing on the barrel. These results are then used to fine-tune the model.

Testing of the barrel with different vibration absorbers is then conducted. Three different versions are used, the differences being the number of rods connecting the mass to the barrel. By varying the number of connecting rods the stiffness, and thus the frequency, of the vibration absorber can be tuned.

For the vibration absorber to be adaptive, this tuning of its frequency should be accomplished without physically changing the rods. Ideally this should be done autonomously or at worst, by selecting a setting from a list. As a first step, a MATLAB® model for an absorber with adjustable stiffness will be presented. Possible ways of making the absorber truly adaptive will be presented.

MATLAB® MODEL

A finite element model of the barrel minus the vibration absorber was created in MATLAB®. Euler-Bernoulli beam approximations and Hermite-cubic interpolation functions are used to form the mass and stiffness matrices for the undamped second order equations of motion by approximating the barrel, a continuous non-uniform beam, as a series of discrete elements. Continuity of lateral displacement and slope are imposed at the element boundaries. When assembled these elements closely approximate the dynamics of the barrel [4].

The geometry of the barrel is entered in 1 mm increments and any non-circular cross sections are smeared together to become circular. This smearing was done to the lugs near the breech end and to the rifling. The mass of the beam is calculated by adding the mass of each of these slices. The actual shape of the beam can be seen in Figure 1. The model's version of this can be seen in Figure 2.

The barrel is just over 2 m long. The muzzle brake was approximated as two hollow cylinders with different interior diameters followed by a hollow cone. The diameters of the cylinders and cones were selected so that both mass and location of the center of gravity matched those of the muzzle brake. A Pro/Engineer® solid model of the muzzle break was used to verify the mass properties.

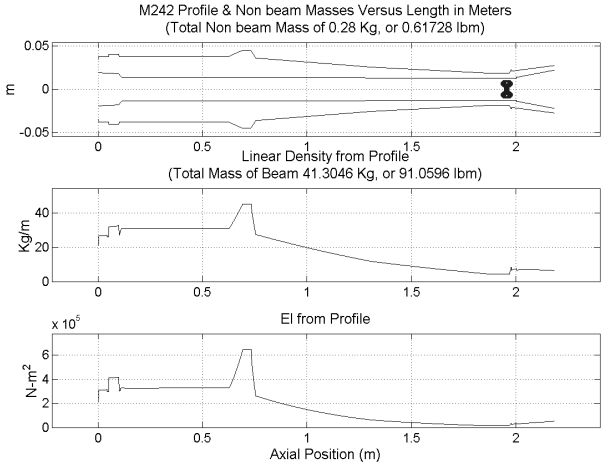

FIGURE 2. BARREL GEOMETRY

After the geometry has been entered the barrel is automatically broken into a user defined number of elements. Nodes are forced to exist at both ends of the barrel and anyplace where constraints are specified. The springs used to hang the barrel during modal testing were entered as constraints in this fashion. The spring constant for the springs was found by hanging weights on them and measuring the deflection.

The other enforced node was at the location of the response accelerometer. This was to allow easy comparison between

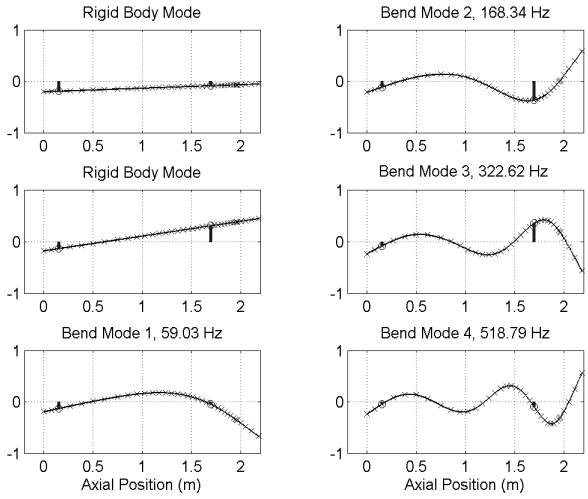

FIGURE 3. DAMPED MODE SHAPES AND NATURAL FREQUENCIES

model and experiment. The mass of the accelerometer was also included and shows up as the dark circles in Figure 2.

Rayleigh proportional damping is used in the model. The values entered were determined in a previous report using this software for analyzing an XM291 gun barrel [1]. After performing an experimental modal analysis on the barrel, experimentally found values were used and the model was rerun. Only minor differences in the resonant frequencies were found.

After the required data was entered the model was run and output generated. The software generates undamped and damped mode shapes and natural frequencies, a pole zero plot of the eigenvalues, time response of the muzzle to a breech impulse, and a bode plot of the muzzle response, plus additional plots about the quality of the FEA analysis. In this case we are interested in the damped mode shapes and natural frequencies. These can be found in Figure 3.

MODAL IMPACT TESTING

After completion of the MATLAB® model, an experimental modal analysis was performed to validate the model. The barrel was hung from two springs to simulate a free-free condition. These springs were contained in the model as mentioned above. This did not present a perfect free-free situation but there is more than an order of magnitude between the highest rigid body mode (1.27 Hz) and the lowest flexible mode (59.03 Hz) so this was deemed satisfactory. Additionally the springs are explicitly represented in the model.

The goal of the modal analysis was to generate a frequency response plot between a force at the breech and the response of the muzzle. For this study an impact was used as the force and the acceleration of the muzzle was the response. An HP 3566A PC Spectrum / Network Analyzer was used to calculate the frequency response. A PCB Impact Hammer with a Delrin tip delivered the impact. The 6 dB roll off point of the tip was found to be 1.605 kHz. A PCB ICP Accelerometer measured the response. The ICP power supply and signal conditioning for both of these was provided by a PCB 12 Channel Rack Mounted Power Unit with a variable gain of 0 to 100 per channel. This set up can be seen in Figure 4.

The HP 3566A was setup with a bandwidth of 800 Hz, 3200 frequency lines and force / exponential windowing. Uniform averaging was performed with a total of 16 averages being used per run. The gain was set to provide good signal strength. After each

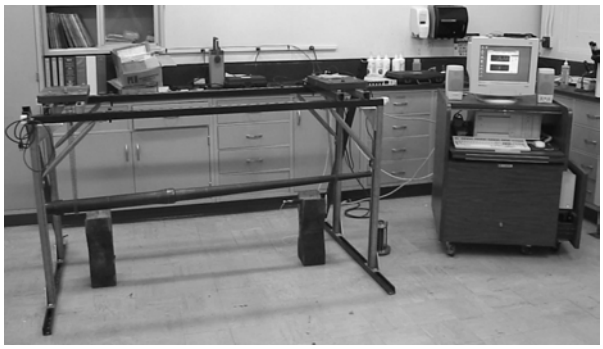

FIGURE 4. EXPERIMENTAL SETUP

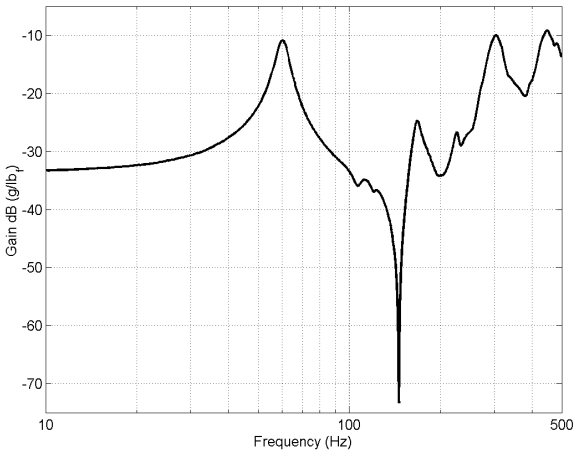

FIGURE 5. PLAIN BARREL – FREQUENCY RESPONSE

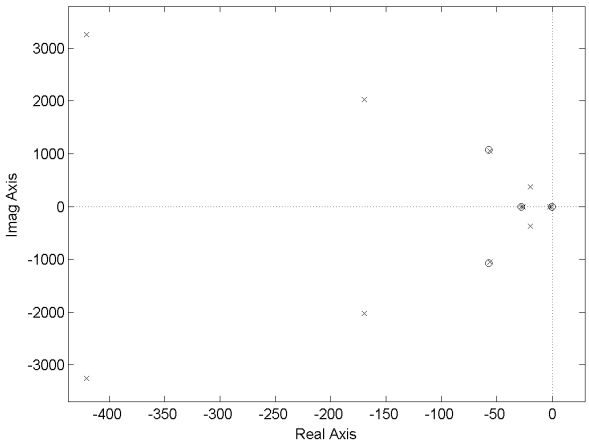

FIGURE 6. POLE-ZERP MAP FOR PLAIN BARREL

impact the data was checked for double hits and overloading of the accelerometer.

The frequency response for barrel can be seen in Figure 5. The first four modes are plainly visible. A collocated pole–zero pair, causes the strange behavior of the second mode. Examination of a pole-zero plot from MATLAB® shows this same behavior. Figure 6 shows this plot for the first four modes and how there is a zero collocated with the second mode.

The Peak Amplitude Method [5] was used to extract the necessary modal parameters from this data. To determine the damping ratio of a peak, equations (1) and (2) were used.

$$\zeta = \frac{1}{2}\eta \tag{1}$$

$$\eta = \frac{1}{2}\frac{\omega_a^2 - \omega_b^2}{\omega_r^2} \tag{2}$$

Where ζ is the viscous damping ratio, η the structural damping loss factor, ω_r is the natural frequency of the peak, and ω_a and ω_b are the half power points. These quantities can be seen in Figure 7.

Once ζ has been found for at least two peaks the proportional damping coefficients, α and β can be found from the following formulas:

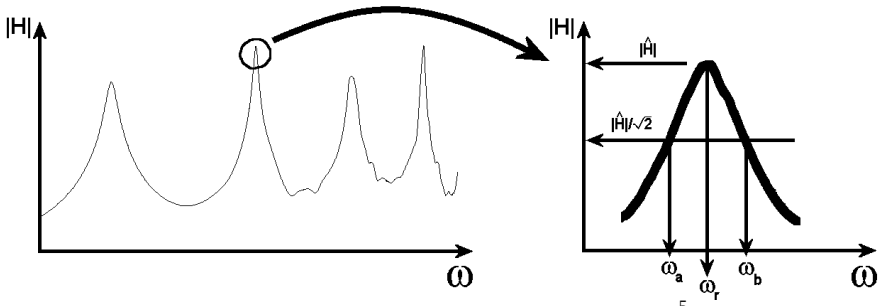

FIGURE 7. PEAK AMPLITUDE METHOD[5]

$$\alpha = -2\frac{\omega_1\omega_2(\omega_1\zeta_2\sqrt{1-\zeta_2^2} - \omega_2\zeta_1\sqrt{1-\zeta_1^2})}{-\omega_1^2 + \omega_1^2\zeta_2^2 - \omega_2^2\zeta_1^2 + \omega_2^2} \tag{3}$$

$$\beta = \frac{-\alpha + \alpha\zeta_2^2 + 2\zeta_2\sqrt{1-\zeta_2^2}\,\omega_2}{\omega_2^2} \tag{4}$$

Using these formulas the following data was found for the three tests shown in Figure 5.

TABLE 1. FREQUENCY RESPONSE PARAMETERS

Plain Barrel with Muzzle Brake				
Peak	**Magnitude**	**Frequency**	**Coherence**	**ζ**
	dB (g/lbf)	Hz		
1	-10.870	60.25	0.9990	0.0456
2	-24.710	167.25	0.9543	0.0361
3	-10.008	304.50	0.9306	
4	-9.117	448.25	0.9314	
α (s-1)	28.428			
β (s)	4.293E-05			

Comparison of this data with Figure 3 shows that the model predicted a stiffer system than was experimentally found. The higher in frequency one goes the more divergent the model and reality become. We are concerned with low frequencies though and the match between the model and experiment is very good for the first two modes. It is only off by about 1 HZ for these modes. This small amount of error is within what was seen from different runs and could be due to the accelerometer mounting and cabling and or the non-ideal connections of the support springs. The measured α and β were put back into the model to see if it would improve results but no appreciable difference was found.

MATLAB® MODEL WITH VIBRATION ABSORBER

Now that the model has been validated for plain barrel it must be modified to include the vibration absorber. The vibration absorber is a proof mass actuator that mounts to the muzzle brake. It consists of a 4.037 lb (1.831 kg) mass, suspended from spring rods, which are attached to a collar, which is in turn press fitted onto the standard muzzle break. The rods are ¼" in (6.35 mm) diameter and extend 5.8" (147.32 mm) from the collar to the mass.

There are three configurations of the vibration absorber: one with eight rods; another with four, two middle one removed top and bottom; and the last with

FIGURE 8. PRO/ENGINEER® MODEL OF THE VIBRATION ABSORBER

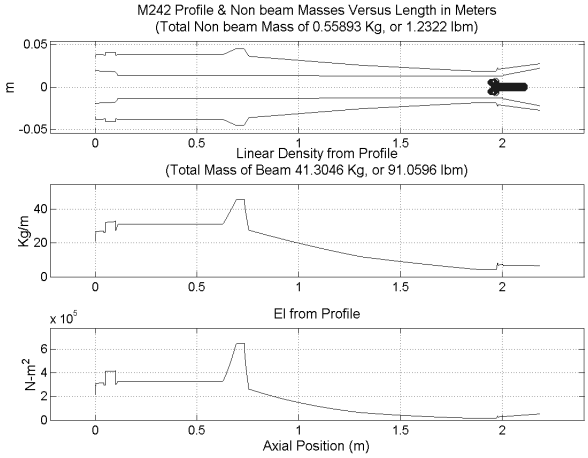

FIGURE 9. BARREL GEOMETRY WITH EIGHT-ROD VIBRATION ABSORBER

two rods oriented diagonally. Only the eight and four rod versions were modeled, using the same number of nodes and enforced node locations as the plain barrel. . The absorber's mounting collar was included by increasing the barrel's outer diameter in that area until the correct mass was added. Since the vibration absorber mounts to the muzzle brake, as before a Pro/Engineer® model was used to ensure that mass and center of gravity location were correct for the entire assembly. Figure 8 shows the model.

The connecting rods were treated as springs and thus by the standard approximation for a spring with mass, 1/3 of their mass was added to the absorber mass and 2/3 was added to the barrel as a lumped mass. The location of the lumped mass was adjusted so as that the center of gravity of the rods and absorber mass together was positioned as in the actual assembly.

The MATLAB® model allows for a mass and stiffness to be entered for a vibration absorber. The mass was a combination of the absorber mass and 1/3 of the rod mass. The stiffness of the absorber was found experimentally by assuming a cantilevered condition between the rods and the mounting collar and then performing a beam bending test. The natural frequencies were found to be 41 Hz and 29 Hz for the eight and four rod versions respectively.

The geometry used by the model for the eight-rod absorber can be seen in Figure 9. The dark area near the muzzle brake is the mass of the accelerometer as before plus the distributed mass of one third of the connecting rods. The only difference between the eight-rod and four-rod versions of the model is the mass of the rods. For the four-rod version the non-beam mass drops to 0.41947 Kg.

As with the plain barrel, the models were run once all required data was entered. Damped mode shapes and natural frequencies were recovered along with bode plots and pole-

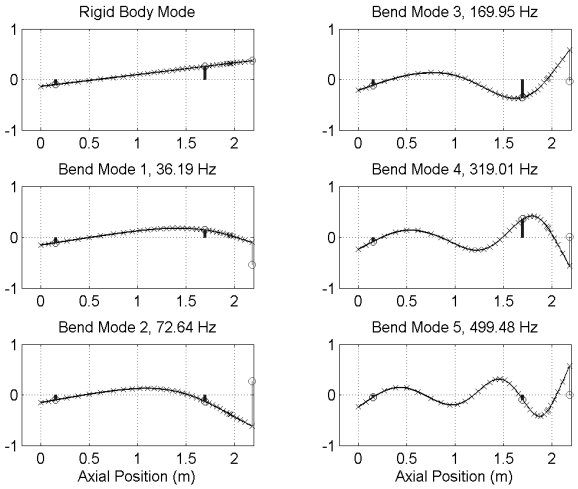

FIGURE 10. DAMPED MODE SHAPES AND NATURAL FREQUENCIES FOR EIGHT-ROD ABSORBER

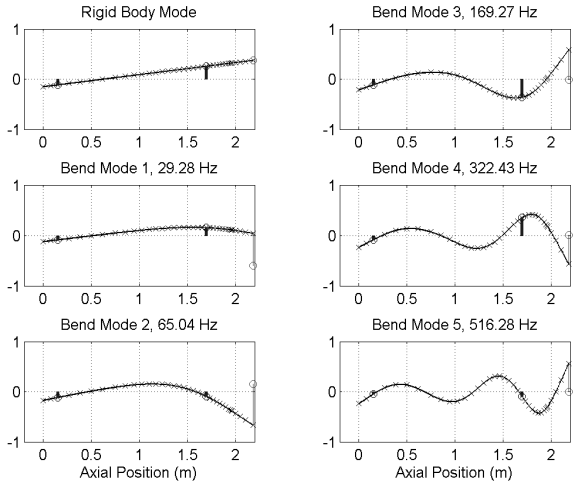

FIGURE 11. DAMPED MODE SHAPES AND NATURAL FREQUENCIES FOR FOUR-ROD ABSORBER

zero maps. The damped mode shapes and natural frequencies can be seen in Figure 10 and Figure 11. The circle at the end of the barrel represents the vibration absorber.

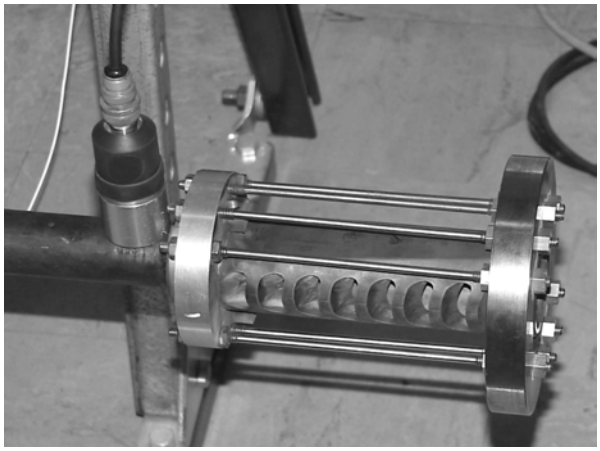

FIGURE 12. INSTALLED VIBRATION ABSORBER

VIBRATION ABSORBER

Now that we have a model including the vibration absorber, modal analyses were done on the different vibration absorber configurations. The barrel orientation and accelerometer placement was kept the same as the last plain barrel test. This ensured that any changes in the frequency response should be directly attributable to the vibration absorber and not changes in test setup.

Three configurations of the vibration absorber were tested, one with eight rods; another with four, two middle one removed top and bottom; and the last with two rods oriented diagonally. The four and eight rod versions were modeled in the previous section. The installed 8-rod absorber can be seen in Figure 12.

The same testing procedure outlined above was used. The rods were removed with the absorber in place so as to minimize any test setup changes between the runs. The absorber was aligned such that the flats of the muzzle brake were parallel to the floor. This is the normal firing position for the cannon. The results of the testing can be seen in Figure 13.

A couple of points are obvious from the plot. First, the major difference between the different configurations is the amount the first peak of the plain barrel is shifted. As fewer rods are installed in the absorber, and thus the absorber stiffness decreases, the first peak moves to progressively lower frequencies. Not only the amount of shift but also the magnitude of the first peak appears to vary with absorber stiffness. At first glance it appears that the eight and four rod vibration absorbers have the same magnitude, with the two rod having a lower magnitude. This will be discussed more when numbers are culled from the data. Lastly, the higher frequency peaks appear to have been largely unchanged.

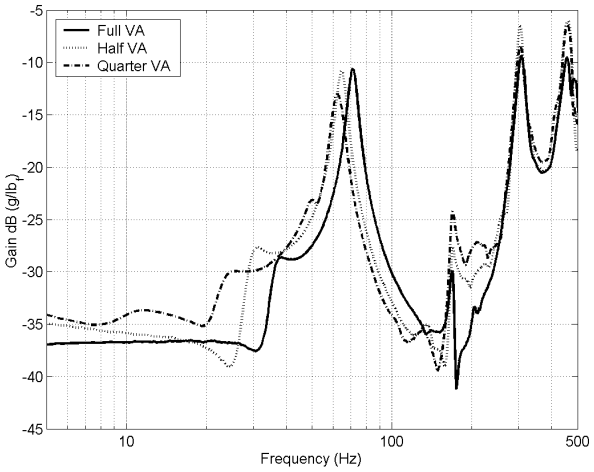

FIGURE 13. VIBRATION ABSORBER – FREQUENCY RESPONSE

If the absorber's frequency coincided with the first peak exactly the peak would have been removed and its energy shifted into the new peaks on either side of it [6]. However we do not have this case so the absorber pushes the peak to a higher frequency. Had the absorber's frequency been above that of the barrel's first mode then it would have pushed the peak to a lower frequency. The additional pole / zero added by the absorber can be seen in the small resonance before the first peak. As stated earlier the strange response at the barrel's second mode is due to a collocated pole-zero pair.

TABLE 2 FREQUENCY RESPONSE PARAMETERS

Full Vibration Absorber			
Peak	**Magnitude**	**Frequency**	**Coherence**
	dB (g/lbf)	Hz	
0	-28.642	38.50	0.9937
1	-10.614	71.25	0.9991
2	-29.886	168.50	0.9887
3	-9.323	307.00	0.9139
4	-9.513	456.25	0.8915
Half Vibration Absorber			
Peak	**Magnitude**	**Frequency**	**Coherence**
	dB (g/lbf)	Hz	
0	-27.683	31.25	0.9998
1	-10.793	64.50	1.0000
2	-27.711	169.75	0.9993
3	-6.541	304.00	0.8724
4	-6.054	460.75	0.8821
Quarter Vibration Absorber			
Peak	**Magnitude**	**Frequency**	**Coherence**
	dB (g/lbf)	Hz	
0	-29.940	25.50	0.9996
1	-13.033	62.50	0.9995
2	-24.251	169.50	0.9777
3	-8.395	304.75	0.8640
4	-6.412	458.50	0.8528

In order to draw more detailed conclusions and to compare to the non-vibration absorber results actual numbers must be removed from the results. The same peak amplitude method was used to pull out this data. The results of this analysis can be seen below in Table 2. The peaks are numbered to coincide with the ones in Table 2, with Peak 0 being the absorbers own peak.

From these numbers it is apparent that the less stiff, i.e. less rods, the vibration absorber is the lower it shifts the first frequency of the barrel. For the higher frequency peaks it appears that the differences seen are due to errors in the data. As far as magnitude goes there appears to be some contradictory data. It appears that the half-absorber produce large magnitude gains than the full but that the quarter absorber produces smaller ones. This could be due to the fact that the quarter absorber no longer has the same cantilever boundary conditions as the other two.

Comparison of this data with Figure 10 and Figure 11 shows that the model overall predicted a stiffer system than was experimentally found. Though the mode of the vibration absorber itself was found to be higher than predicted. This may be due to the way its stiffness was found. The higher in frequency one goes the more divergent the model and reality become. We are primarily concerned with low frequencies though and the match between the model and experiment is very good for the first three modes. It is only off by about 1 HZ for these modes. This small amount of error is within what was seen from different runs and could be due to the accelerometer mounting and cabling and/or the non-ideal connections of the support springs.

COMPARISON

Now that we have looked at the barrel by itself and with a vibration absorber separately it is time to compare the two directly. Figure 14 shows the frequency response of the plain barrel and the three vibration absorber configurations. Figure 15 shows a close up view of the first mode of the barrel.

Examining Figure 14 the two most obvious changes are the shifting of the first mode and the lessening of the zero around 150

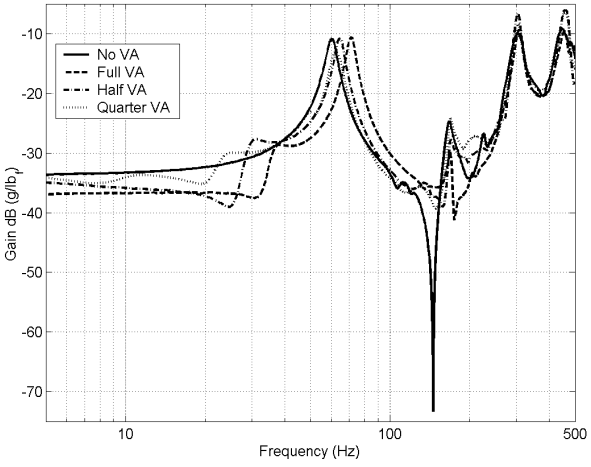

FIGURE 14. FREQUENCY RESPONSE – COMPARISON

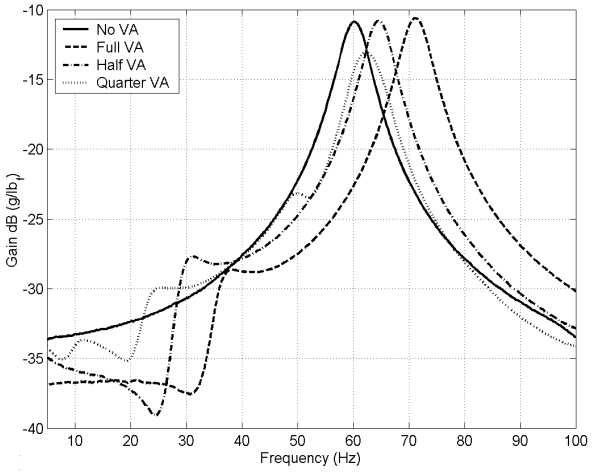

FIGURE 15. FREQUENCY RESPONSE COMPARISON 0 TO 100 HZ

Hz. The higher modes do not appear changed at all. Figure 15 shows the shifting of the first mode more clearly and how the two-rod version is able to reduce the magnitude of the first mode.

Comparing Table 1 and Table 2 one can see that these observations are born out. The second and higher modes are hardly shifted, if at all, while the first one is shifted by as much as 11 Hz. This shifting is what allows the absorber to dampen the system's vibrations. If the system resonance can be shifted away from the disturbance then the vibrations will be reduced.

As stated previously the inclusion of a vibration absorber shifts the modes around it away from its own mode. This accounts for the shifts seen in the barrel's first mode. As part of this shift the absorber can also take energy from the peak it shifts. If the absorber's mode is coincident with one of the system resonances then it would have split the mode and its energy into two smaller resonances.

The two-rod absorber is the only that has an appreciable effect on the magnitude of the barrel's first mode. It reduces the magnitude by almost 3 dB. Due to its different boundary conditions though this may not be as beneficial as it first seems. It could be that it is shifting energy from the vertical plane to the horizontal. Without further testing, it cannot be determined if this drop in the magnitude of the vertical response is beneficial or detrimental to system performance. An increase in horizontal motion would not be beneficial.

MATLAB® MODEL – VARIABLE STIFFNESS ABSORBER

As a first step towards an adaptive absorber it must be determined if any advantages can be achieved by adjusting the stiffness of the vibration absorber. If the same level of performance gains are achievable with a fixed stiffness vibration absorber than there is no need undertake making the absorber adaptive. To undertake this study the absorber models created earlier are rerun with different values used for the absorber's stiffness. Being able to change the stiffness while leaving the other properties the same would allow for the absorber to be tuned for various operating conditions.

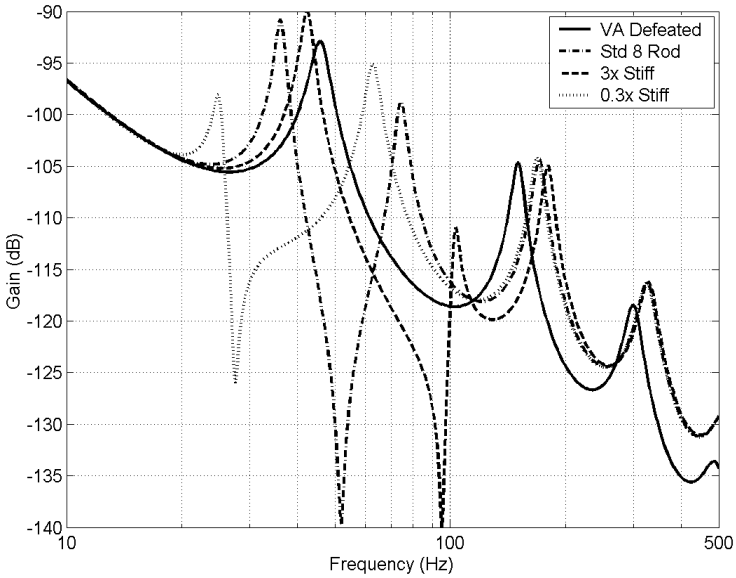

FIGURE 16. POINTING ANGLE FREQUENCY RESPONSE FOR DIFFERENT STIFFNESS 8 – ROD ABOSORBERS

Frequency response functions for the pointing angles of the muzzle were calculated for different configurations. The configurations included the absorbers as tested, with their stiffness increased by a factor of 3, and with their stiffness decreased by a factor of 3. Additionally a defeated version of the eight-rod absorber was modeled. The defeated absorber models the absorber as simply a mass on the end of the barrel. This allows us to see whether the changes in the frequency response are simply due to the additional mass.

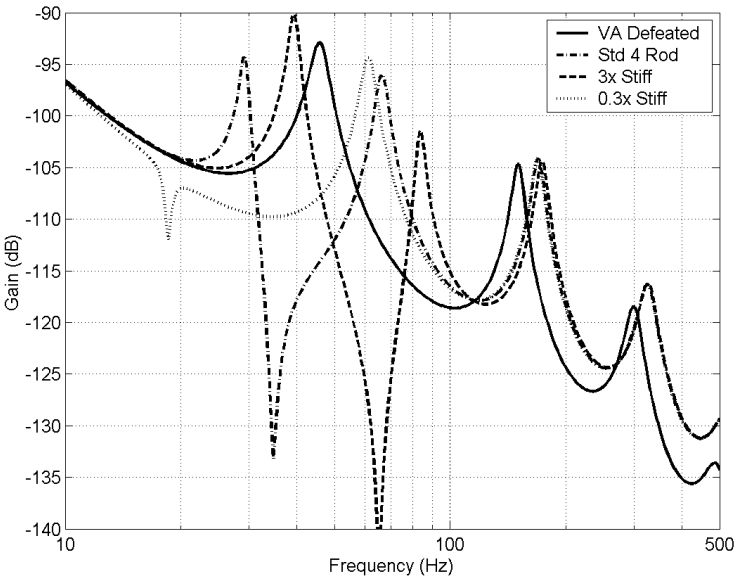

FIGURE 17. POINTING ANGLE FREQUENCY RESPONSE FOR DIFFERENT STIFFNESS 4 – ROD ABSORBERS

Figure 16 shows the results for the eight-rod absorber variant and Figure 17 does the same for the four rod ones. It is apparent from these figures that the ability to change the stiffness can greatly affect the response of the system. By increasing the stiffness of the four-rod we can make it perform similar to the eight rod. Conversely, by decreasing the stiffness of the eight-rod we can make it perform like the four rod one. All of these changes though only effect the response greatly below 100 Hz. Above there they all perform similarly and are appear as versions of the defeated absorber shifted to higher frequencies.

Which version of the absorber is best depends upon the operating conditions. Careful inspection of the figures shows that each has a range of frequencies over which they offer significantly reduced response compared to the defeated absorber. The eight-rod version of the absorber has been fired and shown to cut shot dispersion in half [7]. However this was under only one set of operating conditions. Looking at the responses, it is apparent that there are areas where the other absorbers outperform the eight rod one. Thus if the operating conditions change to an area where an eight rod absorber with a different stiffness is superior being able to change this stiffness would yield an increase in performance.

MAKING THE ABSORBER ADAPTIVE

Now that we have seen that performance gains can be achieved by making the absorber adaptive how can this actually be accomplished? In the previous section we changed the stiffness of the absorber to effect the desired change in frequency. In the laboratory experiments we changed the stiffness by removing rods. Obviously this is not a satisfactory way to make the absorber adaptive. For the absorber to be adaptive the stiffness change should be accomplished rapidly and without need for gross mechanical modifications like removing rods.

This type of application lends itself to active materials. Materials such as shape memory alloys, piezoceramics, or other induced strain actuators are designed for such applications. If only a few natural frequencies and large changes in stiffness are desired then shape memory

alloys are a natural choice. If a range of natural frequencies is desired then piezoceramics may be a better choice. Piezoelectrics also may be useful for eliminating high frequency modes.

Which type of actuator to utilize would depend upon the desired change. The perfect solution may actually contain different types of actuators all working together. The previous section showed the types of changes that could be achieved by increasing or decreasing the stiffness by a factor of three. The changes were concentrated in the low frequency (below 100 Hz) regime. If these types of changes are desired then shape memory alloys (SMA) become a logical choice as their Young's modulus can change by a factor of three when going from martensite to austenite [8].

There are a couple of different ways in which SMAs can be used to make the absorber adaptive. The most direct way would be to replace the existing spring rods with hybrid SMA rods. The core of the rods would be stainless and would be just large enough to withstand the axial loads. The rest of the rod would be SMA and would take care of the bending loads. Thus when activated an immediate factor of three in the modulus of the rods could be achieved. Since the stiffness of the rods is directly proportional to its Young's modulus, this would translate directly into an increase in stiffness.

Another possible way of using SMA to achieve a stiffness change would be in the connections between the spring rods and the collar. If SMA inserts were used as part of the connection, they could be used to loosen or tighten the connection. If the connection was loosened then the rods would able to deflect more for a given applied force. Conversely if the connection was tightened the rods would deflect less. Since the stiffness of the absorber can be viewed as how far the rods will deflect under a given load, a change in the connection would manifest itself as a change in the apparent stiffness of the absorber.

SMAs are bistable so they are most useful when there are only two desired operating points, the base one being when the SMA is in its martensite phase and the second when it is in its austentite phase. For the M242 there are two operating speeds so this does not appear to pose a problem. However if more than two operating points were desired then it might be possible to achieve them by only operating some of the SMA actuators. This is something that would have to be considered during the design of the absorber.

CONCLUSIONS

This paper has shown the effect of mounting a vibration absorber to the muzzle brake of an M242 Bushmaster. A MATLAB® model of the barrel was developed and then verified by performing modal impact testing upon the actual barrel. Good agreement was found between the model and experimental data.

After modeling and testing the plain barrel a vibration absorber was modeled and tested to find its effects upon the barrels frequency response. Two different configurations were modeled, while three were tested. As with the plain barrel good agreement was found between the model and reality. It was found that the absorber shifted the first resonant frequency of the barrel higher in frequency and that the two-rod version of the absorber reduced the magnitude of the response by 3 dB.

It was shown that changing the absorber's stiffness could change its frequency response. Which version of the absorber is best would depend upon the operating conditions. Through the

use of active materials the absorber could be made adaptive and thus able to handle different operating conditions with out physically changing the absorbers configuration.

Overall it was shown that by mounting a proof mass type actuator on the muzzle brake, the performance of the gun system could be increased. Since this is a part of the barrel meant to be screwed on and off, this allows for very easy mounting without affecting the rest of the gun system.

An additional advantage of mounting the absorber to the muzzle is that its mass ring may be combined with a muzzle fuse set device [9]. Previously a drawback of such devices was that they increased the weight affixed to the muzzle brake. Combining it with the absorber allows for its additional mass to be used to improve the gun's accuracy

REFERENCES

1 Kathe, E., "Design and Validation of a Gun Barrel Vibration Absorber Proceedings of the 67th Shock and Vibration Symposium: Volume 1, Published by SAVIAC, Monterey, CA, 18-22 November 1996, pp. 447-456.

2 Kathe, E., "A Gun Barrel Vibration Absorber for Weapon Platforms Subject to Environmental Vibrations," *AIAA Paper No. 98-1846, A Collection of Technical Papers – 39th AIAA/ASME/ASCHE/AHS/ASC Structures, Structural Dynamics, and Materials Conference and Exhibit and AIAA/ASME/AHS Adaptive Structures Forum*, 1998, pp.1284-1294.

3 Kathe, E., "Gun Barrel Vibration Absorber," US Patent 6167794, January 2001.

4 Kathe, E., "MATLAB® Modeling of Non-Uniform Beams Using the Finite Element Method for Dynamics Design and Analysis," U.S. Army ARDEC Report, ARCCB-TR-96010, Benét Laboratories, Watervliet, NY, April 1996.

5 Ewins, D. J., "Modal Testing: Theory, Practice and Application," Research Studies Press, Ltd., Baldock, England, 2000.

6 Den Hartog, J. P., "Mechanical Vibrations," McGraw-Hill Book Company, Inc., New York, 1956.

7 Kathe, E., "Lessons Learned on the Application of Vibration Absorbers for Enhanced Cannon Stabilization," Proceedings of the Eighth U.S. Army Symposium on Gun Dynamics, Eric Kathe Ed., ARDEC, CCAC, Benét Technical Report ARCCB-SP-99015, Mc Lean, VA, 17-19 Nov 1998, pp10-1 – 10-15.

8 NASA Technical Memorandum 107861, "A State of the Art Assessment of Active Structures," Sept 1992.

9 Freymond, P. H., and Buckley, A., "Programmable Fuzing for Tube Launched Ammunition," NDIA 35th Annual Gun & Ammunition Symposium, Williamsburg, VA, May 2000.